Bulletin of the Seismological Society of America, Vol. 96, No. 2, pp. 722–728, April 2006, doi: 10.1785/0120050146

Obtaining Absolute Locations for Quarry Seismicity Using Remote Sensing Data

by Guoqing Lin, Peter Shearer, and Yuri Fialko

Abstract We obtain absolute locations for 19 clusters of mining-induced seismicity in southern California by identifying quarries using remote sensing data, including optical imagery and differential digital elevation models. These seismicity clusters contain 16,574 events from the Southern California Seismic Network from 1984 to 2002, which are flagged as quarry blasts but without any ground-truth location constraints. Using georeferenced airphotos and satellite radar topography data, we identify the likely sources of these events as quarries that are clearly visible within 1 to 2 km of the seismically determined locations. We then shift the clusters to align with the airphoto images, obtaining an estimated absolute location accuracy of ~200 m for the cluster centroids. The improved locations of these explosions should be helpful for constraining regional 3D velocity models.

Introduction

Because of the trade-off between earthquake locations and velocity structure in the tomography problem, controlled sources are often used in velocity inversions to provide absolute reference locations for 3D velocity models and to constrain the shallow crustal structure. Ideally these are calibration shots of known locations and origin times. Quarry blasts are also sometimes used, however, which typically have known locations but unknown origin times. When included in the location algorithms, the hypocentral parameters of these controlled sources (locations and/or origin times) are fixed.

Absolute location information is typically available for only a fraction of the artificial sources located by local and regional networks. For example, the Southern California Seismic Network (SCSN) lists 23,748 events from 1984 to 2002 as shots or quarry blasts, but only 77 of these have true location information (E. Hauksson, personal comm., 2005). Here, we demonstrate with SCSN events how remote sensing data (air or satellite photos and digital elevation maps) can be used to determine the absolute locations of quarry seismicity clusters to about 200 m accuracy. The results produce a check on catalog location accuracy as well as new constraints for the tomography problem.

Method

We use as our starting point the SHLK location catalog (Shearer *et al.*, 2003, 2005), which contains precise relative relocations for more than 340,000 southern California earthquakes that occurred between 1984 and 2002, as computed by the source-specific station term, waveform cross-correlation, and cluster analysis methods. The relative location errors are estimated from the internal consistency of differential locations between individual event pairs and are often as small as tens of meters. Because of imprecise knowledge of the 3D velocity structure, however, the absolute locations of seismicity clusters are much worse constrained, with location errors as large as a few kilometers.

The SCSN flags 23,748 events as quarry blasts in southern California between 1984 and 2002 (see Fig. 1). As noted by Agnew (1990), Richards-Dinger and Shearer (2000), and Wiemer and Baer (2000), artificial seismicity can also be identified using comparisons of daytime versus nighttime seismic activity. However, we find that the quarry blast list from the SCSN catalog is more complete than that derived from a simple analysis of the diurnal seismicity patterns. We therefore use the SCSN-defined blast data in this study. The red dots in Figure 1 represent the 16,574 events that we are able to relocate. For other events, we could not find suitable airphoto images or identify unambiguous source locations. In many cases, the corresponding events represent distributed explosions associated with road construction or military bombing ranges.

We estimate the true locations of the quarry blasts from airphoto images provided by AirPhoto USA (available at http://terraserver.com/). AirPhoto USA's catalog consists of recent, true-color, high-resolution aerial photography of many regions in the United States. The resolution of the images used in this study is typically 8 m but can be as small as 0.6 m. Figure 2 illustrates our method as applied to cluster 11 in Figure 1. Figure 2a is a closeup of the cluster events as seismically located in the SHLK catalog. Figure 2b shows the corresponding airphoto image in the same coordinate

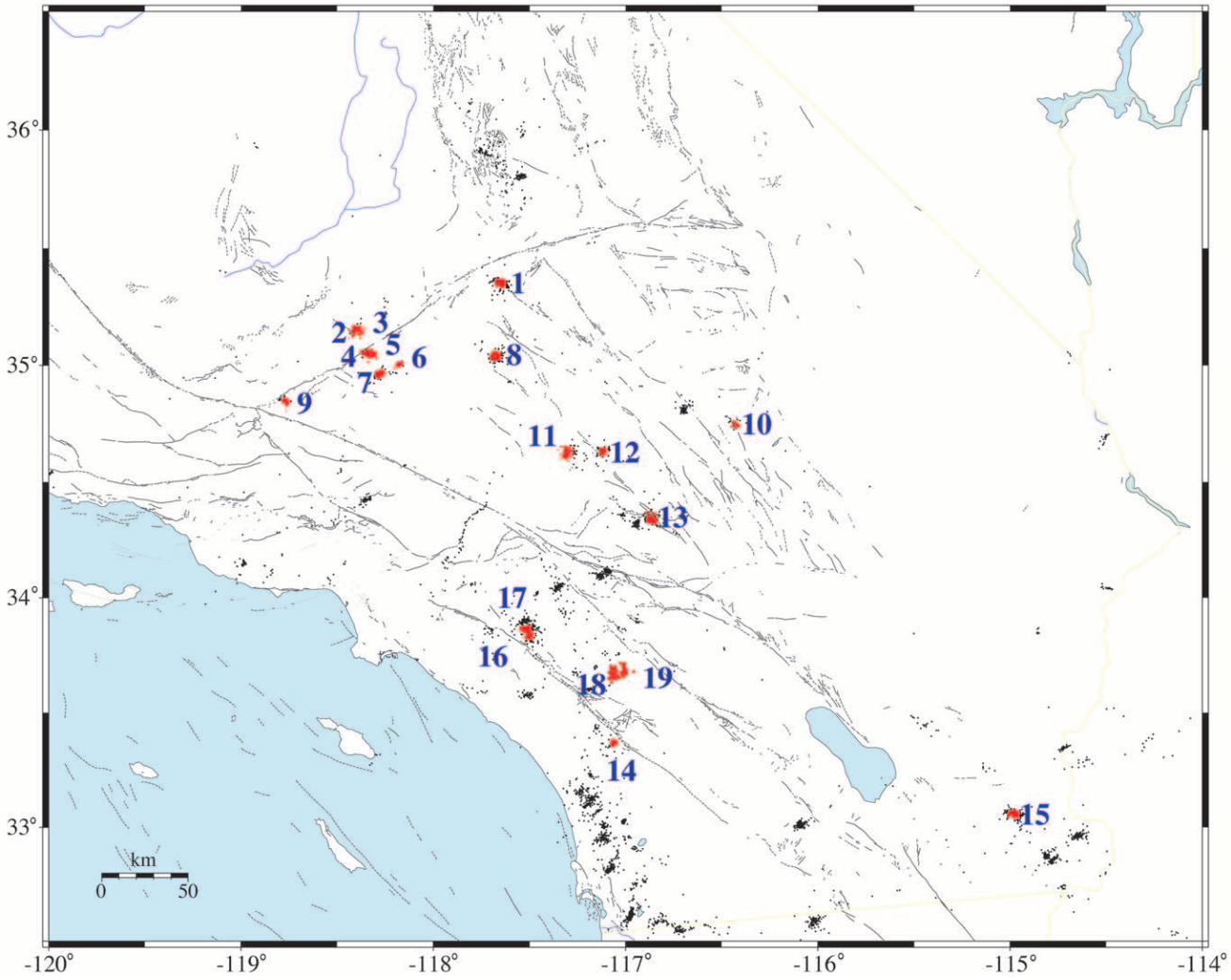

Figure 1. Map view of the 23,478 quarry blasts flagged by the Southern California Seismic Network (SCSN) between 1984 and 2002 in southern California plotted at their SHLK catalog locations. The red dots represent the seismicity clusters that we are able to relocate using airphoto or satellite images. Also shown are the numbers used to identify the respective clusters in our study. Gray lines denote active Quaternary faults.

frame. The ground resolution of this image is 8 m. The disturbed terrain near the top right corner shows a quarry that is the obvious source of seismicity, but the quarry location is about 0.8 km southwest of the seismicity cluster.

To verify that the quarry is indeed the source of seismic activity, we have analyzed changes in the Earth's topography using digital elevation model (DEM) data from the National Elevation Dataset (NED, http://ned.usgs.gov) and the Shuttle Radar Topography Mission (SRTM) (Farr and Kobrick, 2000). The SRTM data were collected in 2000, whereas the NED data represent a compilation from various measurements conducted between 1925 and 1999. The vertical accuracy of both DEMs is of the order of 10 m. Therefore a systematic difference between the two DEMs that exceeds 10 m is indicative of changes in the surface elevation that occurred between the acquisition dates of the respective DEMs. Figure 2c shows a differential DEM for the same area as in Figure 2a and b. White regions in Figure 2c denote areas where the elevation has decreased by more than 20 m, presumably because of ground excavation. The location of the area of a decrease in surface elevation agrees with the quarry location inferred from the optical imagery (Fig. 2b). The horizontal resolution of the digital topography data is 30 m. Our approach is to use the airphoto images to locate probable quarries and differential DEM to confirm that these features are associated with the removal of a significant volume of material. The remote sensing data alone cannot determine when the quarries were active, but it seems likely that the observed events (flagged in the SCSN catalog as quarry blasts) are caused by explosions at these sites.

Next, we compare Figure 2a and b and shift the entire seismicity cluster to align with the imaged quarry as shown in Figure 2d. The blue arrow gives the mislocation vector for the cluster, the location shift from our estimated true

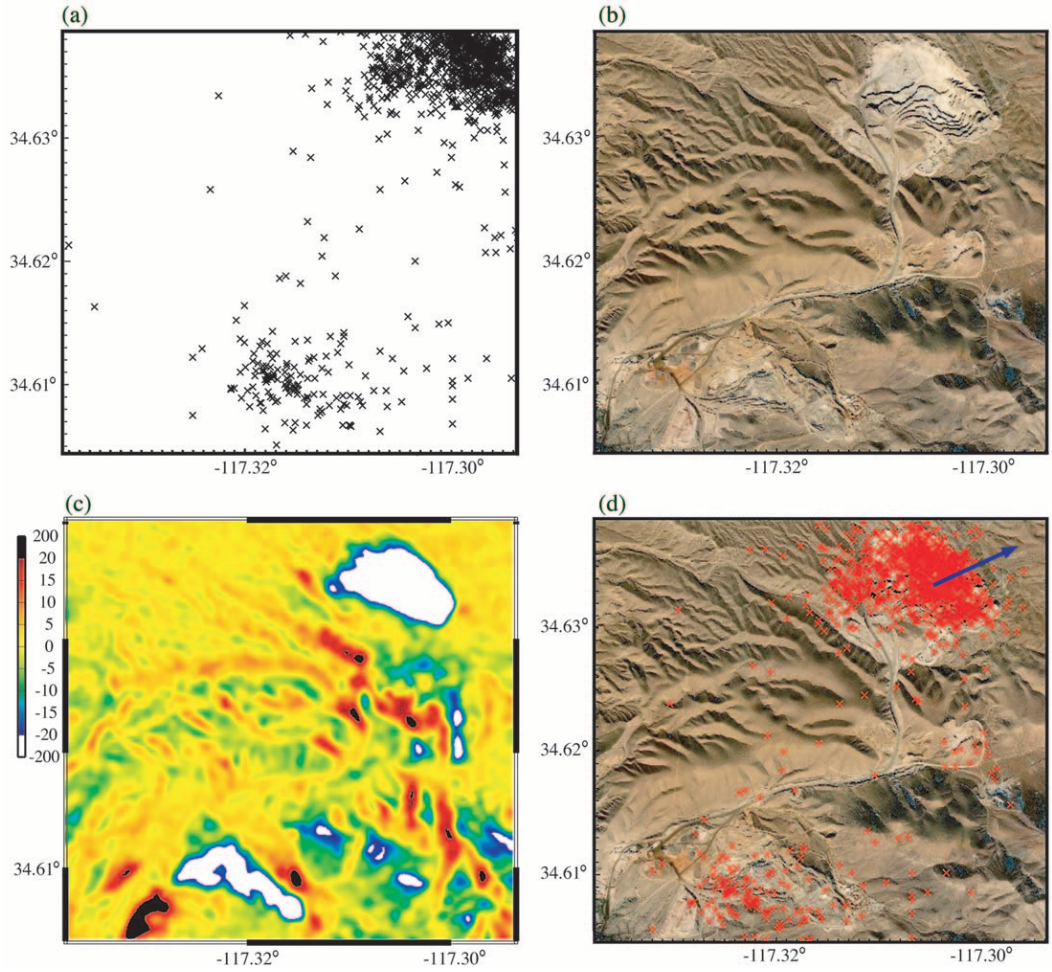

Figure 2. Details of relocation method for cluster 11. (a) The starting SHLK seismicity clusters. (b) The airphoto image corresponding to the clusters in (a). (c) The differential DEM data plot for the same area. Positive changes (red) represent topography increases and negative changes (blue) represent topography decreases. The most extreme changes are shown in black and white. The white spots are likely quarries, confirming their locations as shown in (b). (d) The shifted clusters together with the airphoto image. The arrow shows the mislocation vector from the estimated true locations to the starting SHLK locations.

location to the SHLK location. Note that this is opposite to the direction that we shift the SHLK cluster to align with the quarry image. Notice that the ~1 km width of the quarry indicates that most of the scatter shown in the SHLK locations is real; this is consistent with the relative event location accuracy among nearby events being much better than the absolute location accuracy of the entire cluster. There is some subjectivity in determining the best shift of the seismicity clusters; in general, we attempt to visually align the cluster centroid with the center of the quarry shown in the airphoto but in some cases irregularities in the quarry shape provide a better alignment method. Further refinements might be possible by studying the time evolution of the quarries by examining airphotos at different dates and comparing them with the seismic results, but we do not attempt this here.

Notice that several smaller quarries are visible to the southwest of the main quarry, one of which is associated with its own seismicity cloud. In this case, the alignment obtained for the main quarry appears to also roughly align the secondary quarry, so we do not perform a separate alignment of the secondary quarry. This is again consistent with the much smaller relative relocation error, even between different clusters, compared with absolute location error for the SHLK catalog. In other cases, however, nearby quarries appear to have significantly different mislocation vectors, even when the quarries are only a few kilometers apart. Thus, we perform separate alignments for the cluster pairs 2–3, 4–5, 16–17, and 18–19.

Additional examples of our method are included in Figures 3 and 4 for clusters 3 and 5 (see Fig. 1), respectively. In these examples, secondary quarries visible in the same

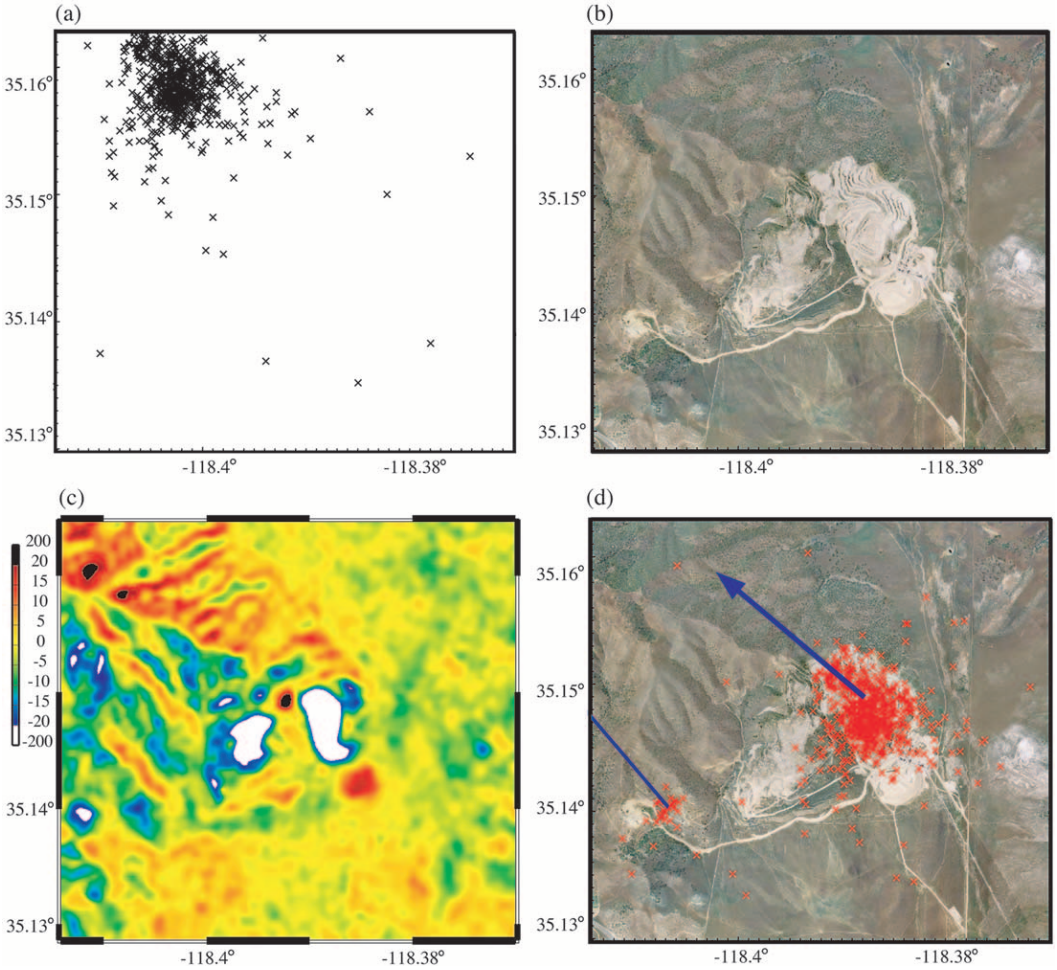

Figure 3. Application of relocation method for cluster 3. Notation is the same as in Figure 2. There is a small cluster on the left side of (d) with the mislocation vector, which is cluster 2 in Figure 5. These two clusters are relocated separately because the mislocation vectors are different. (For more details, please refer to the text.)

images are used to separately locate clusters 2 and 4 in Figure 1. Figure 5 presents all 19 clusters that we relocated using the optical images in our study. The arrows show the directions of the mislocation vectors with the size proportional to the distance from the true locations (red dots) to the initial SHLK locations (black dots). Figure 6 shows the mislocation vectors mapped onto the quarry locations. Note that the scale for the arrow length is increased compared with the map scale to make the arrows visible. The location errors for all the clusters in our study are less than 2.1 km, with most errors being less than 1 km. This implies that the absolute horizontal location error of the SHLK catalog is generally less than 1 km but can be as much as 2 km. Depth errors can also be evaluated because the SCSN restricts the quarry blasts to be at the surface, whereas the SHLK locations for all event types are allowed to have nonzero depths. The SHLK catalog median depths for the mining-induced clusters in this study range from 0.7 to 3.6 km, with most between 1.2 and 2.4 km. This implies that the SHLK catalog depth errors for shallow events are greater than their horizontal errors, but, in general, are less than 2.5 km.

Discussion

These results provide additional ground-truth events that can be used to test the accuracy of the catalog locations and remove some of the trade-offs between the event locations and 3D velocity structure in tomographic inversions. The bias in seismically located quarry blasts compared with their true locations exhibits some spatial coherence. For example, clusters 2 to 7 are all biased northwest of their true locations, whereas clusters 1 and 8 are biased eastward of their true locations. Additional information on the location bias is provided by the controlled-source data. Figure 7 shows that the controlled-source mislocation vectors are generally consistent with the new mislocation vectors obtained in this study; they typically have a magnitude of 1 to 2 km and roughly agree in direction among nearby clusters.

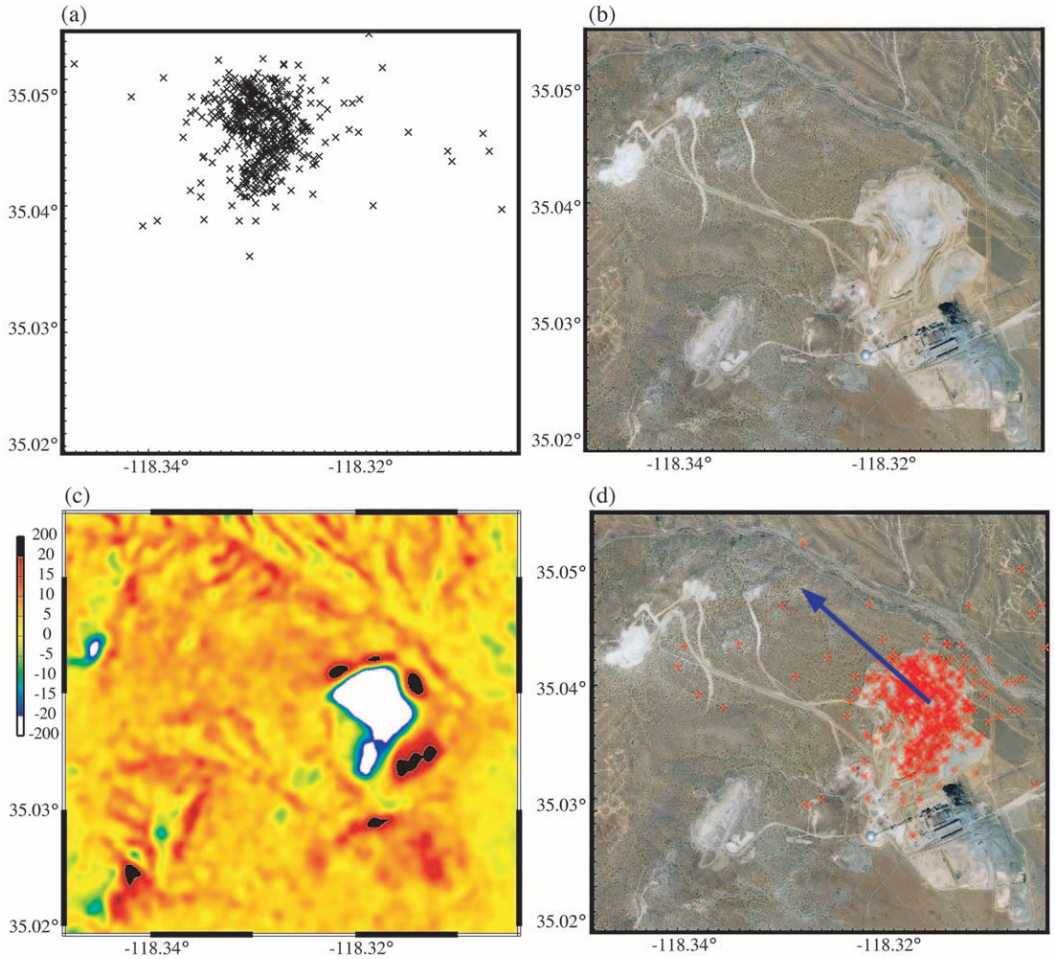

Figure 4. Application of relocation method for cluster 5. Notation is the same as in Figure 2.

Significant variability occurs in the results, however, even among clusters separated by only a few kilometers, implying that the near-surface velocity structure is a substantial contributor to the location error. Thus, direct removal of location bias by using calibration events of known location is guaranteed to work well only when the calibration event is quite close to the target events. Even with our new results, the calibration event coverage is too sparse to provide reliable mislocation bias estimates for many regions. Details of the mislocation bias will also be hard to completely resolve with 3D velocity inversions because of their limited spatial resolution compared with the length scale of the variations shown in Figure 7.

Despite these limitations, our new results represent a substantial improvement over existing controlled-source information for southern California and should help to provide better constrained tomography models and absolute earthquake locations. Note that most of the quarries that we study are active operations, for which detailed information could probably be obtained by contacting the quarry operators. The advantage of our approach is that quarry locations can be obtained directly from freely available remote sensing data sets, without the need for any other research, correspondence, or site visits.

Acknowledgments

We thank Egill Hauksson who provided the controlled-source locations and times and Duncan Agnew for useful suggestions. We also thank Paul Wessel and Walter Smith for developing and supporting the GMT mapping tools (http://gmt.soest.hawaii.edu/). Funding for this research was provided by National Earthquake Hazards Reduction Program/U.S. Geological Survey (USGS) grant 03HQPA0001. This research was also supported by the Southern California Earthquake Center, which is funded by National Science Foundation Cooperative Agreement EAR-0106924 and USGS Cooperative Agreement 02HQAG0008. The Southern California Earthquake Center contribution number for this article is 914.

References

Agnew, D. (1990). The use of time-of-day seismicity maps for earthquake/explosion discrimination by local networks, with an application to the seismicity of San Diego county, *Bull. Seism. Soc. Am.* **80,** 747–750.

Farr, T. G., and M. Kobrick (2000). Shuttle radar topography mission produces a wealth of data, *AGU EOS* **81,** 583–585.

Richards-Dinger, K., and P. Shearer (2000). Earthquake locations in south-

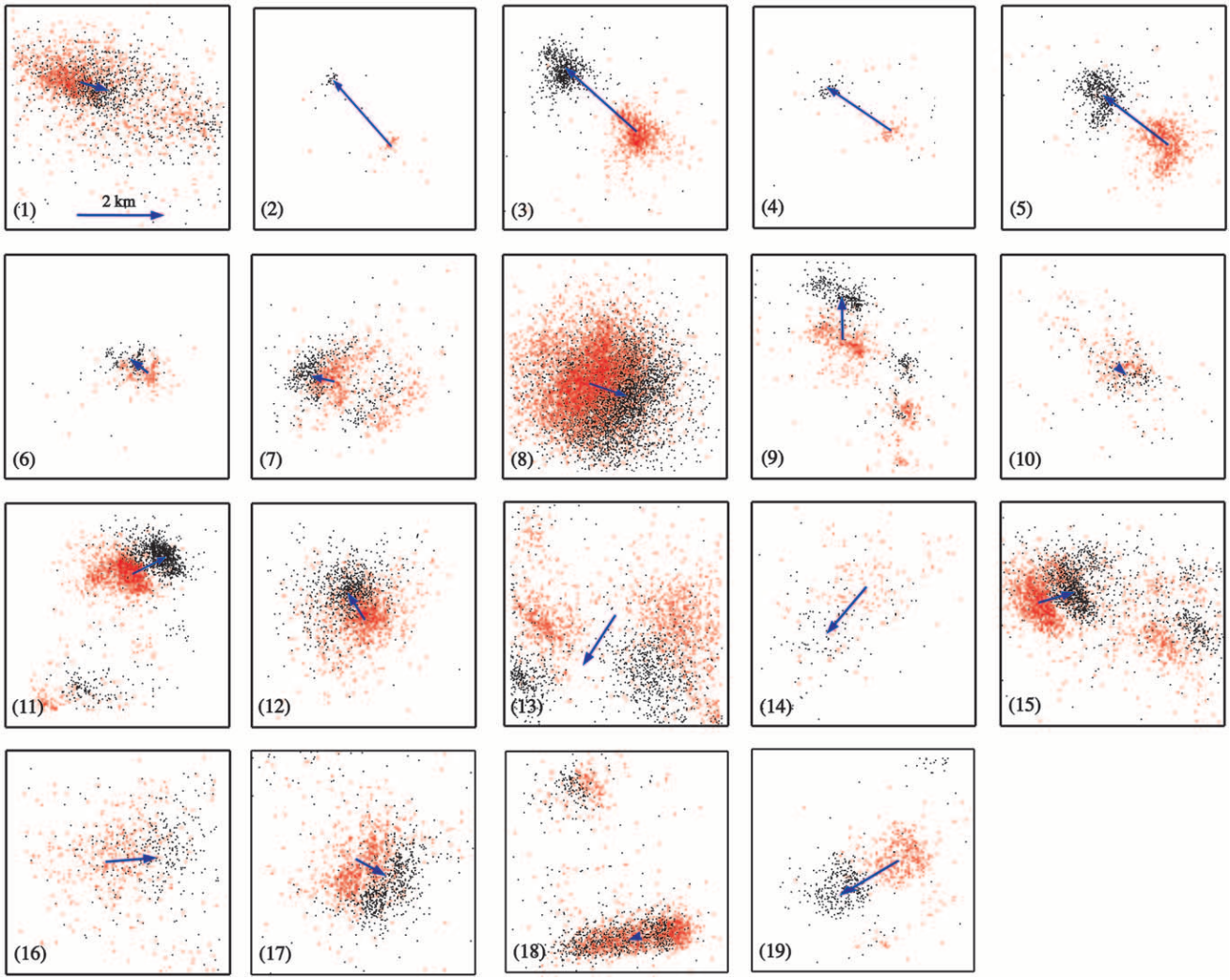

Figure 5. The 19 quarry blast clusters examined in our study. The black dots represent the starting SHLK catalog locations, and the red dots represent the improved (shifted) locations. The arrows show the mislocation vectors with the size proportional to the distance from the estimated true locations to the starting SHLK locations. The magnitude of the location changes for all the clusters in our study is less than 2.1 km, implying that the absolute location errors in the SHLK catalog are roughly 1 to 2 km.

ern California obtained using source-specific station terms, *J. Geophys. Res.* **105,** 10,939–10,960.

Shearer, P., E. Hauksson, and G. Lin (2005). Southern California hypocenter relocation with waveform cross-correlation, part 2: results using source-specific station terms and cluster analysis, *Bull. Seism. Soc. Am.* **95,** 904–915.

Shearer, P., E. Hauksson, G. Lin, and D. Kilb (2003). Comprehensive waveform cross-correlation of southern California seismograms: Part 2. Event locations obtained using cluster analysis, *EOS Trans. AGU* **84,** no. 46, Fall Meet. Suppl., Abstract S21D-0326.

Wiemer, S., and M. Baer (2000). Mapping and removing quarry blast events from seismicity catalogs, *Bull. Seism. Soc. Am.* **90,** no. 2, 525–530.

Institute of Geophysics and Planetary Physics
University of California San Diego
La Jolla, California 92093
gulin@ucsd.edu
pshearer@ucsd.edu
yfialko@ucsd.edu

Manuscript received 21 July 2005.

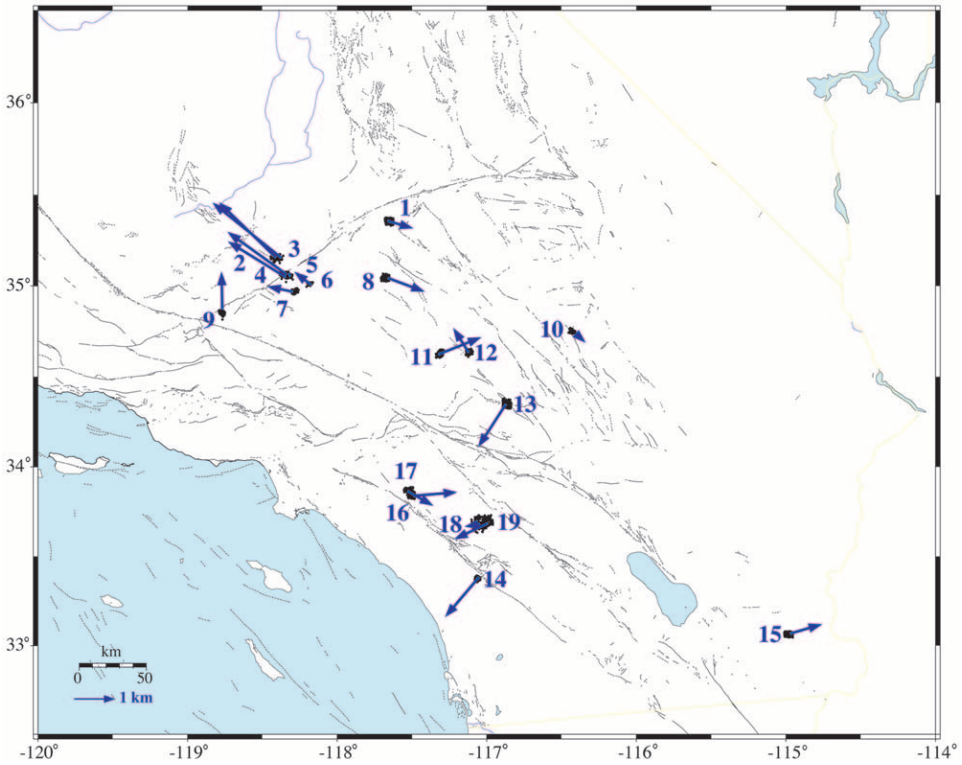

Figure 6. The locations of the 19 quarry blast clusters in southern California used in our study. The arrows show the mislocation vectors with the size proportional to the distance from the estimated true locations to the starting SHLK locations. Note the difference between the arrow scale and the map scale.

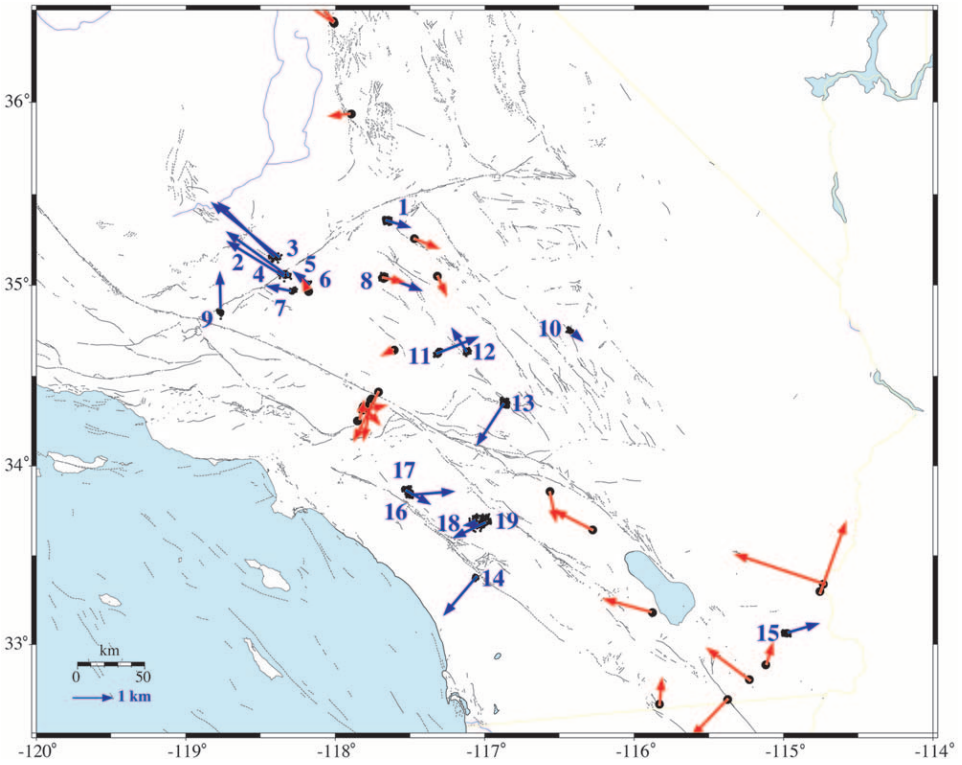

Figure 7. The locations of both the 19 quarry seismicity clusters used in our study (blue arrows) and some controlled sources with known locations (red arrows). The arrows show the mislocation vectors with the size proportional to the distance from the estimated true locations to the starting SHLK locations. Note the difference between the arrow scale and the map scale.